LRP 826/06 October 2006

Low cycle fatigue and creep-fatigue of Eurofer 97

EFDA Technology Workprogramme 2003
Final Report on task TW3-TTMS-005/Del No. 1

P. Marmy

ISSN 0458-5895

Centre de Recherche en Physique des Plasmas,
Technologie de la fusion
Association Euratom-Confédération Suisse
Ecole Polytechnique fédérale de Lausanne
5232 Villigen, PSI, Switzerland

Low Cycle Fatigue and Creep-Fatigue of Eurofer 97

EFDA Technology Workprogramme 2003

Final Report on task

TW3-TTMS-005 / Del No. 1

P. Marmy

Mai 2006

1. Introduction

The 9-12% Cr ferritic-martensitic steels are being presently considered as main candidate materials for the first wall components of future fusion reactors. Recent developments are focussed on the chemical composition to achieve low activation and fast decay properties after irradiation (so called RAFM steels) as well as on the reduction of the shift of the ductile-brittle transition temperature after irradiation.

In the European Union, in the frame of the Long Term Programme of EFDA, an optimized composition of RAFM steel has been designed and produced, based on previous steel developments known as MANET, CETA, OPTIFER, OPTIMAX and F82H[1-3] . The steel was given the name EUROFER 97.

Since fusion reactors will be run cyclically, fatigue and creep fatigue properties are needed as a basic input for designers. Up to now, published data on the fatigue properties of Eurofer 97 are scarce (see for instance [4, 5]or report NRG 20023/05.68497/P) .The aim of this work is to investigate the low cycle fatigue (LCF) and creep fatigue properties of EUROFER 97 at elevated temperatures but also to collect preliminary information on the fatigue behaviour of the new material. The first part of the work is a simple investigation of the room temperature low cycle fatigue properties. Fatigue tests were then carried out at different temperatures as described in the task proposal, at RT, 150, 300,350 and 550°C. Finally a series of creep-fatigue tests was carried out, imposing a 500 sec dwell at the maximum tensile strain of the loading cycle.

2. Material

The material used in this study is the European reference steel EUROFER 97, produced by the Böhler Edelstahl company under the name Z-T512.
The heat number of the steel is E83697 and according to the inspection certificate, the material was delivered from material under POS 30, Plate no.2, subdivided in 15 plates 2/1 to 2/15. The specimens were cut from plate number 2/15, in the longitudinal direction. The plate thickness was 25mm.

The chemical analysis is as follows (Böhler Inspection Certificate 3.1B):

C	Si	Mn	P	S	Cr	Mo	V	W	Ti	N
0.12	0.06	0.47	<0.005	0.004	8.96	<0.001	0.2	1.08	0.006	0.021

Ni	Cu	Co	Al	Nb	B	Ta	O	As	Sn
0.022	0.0036	0.007	0.008	0.0022	<0.0010	0.14	0.0012	<0.005	<0.005

Zr	Sb
<0.005	<0.005

The alloy is molybdenum , nickel and niobium free, to achieve fast decay properties. The chromium content is around 9% to ensure a full martensitic transformation at room temperature. The Mn concentration is relatively high (0.5%) to avoid the formation of delta ferrite. Ta is present (0.14%) to reduce prior austenite grain growth. Va is also added as a strong carbide former.

The heat treatment given to the plate was:

Austenitization at 980°C for 30.6 min and air cooling
Tempering at 760°C for 1.5 hr and air cooling

The steel is then reported to have a grain size of 9 (ASTM) and a delta ferrite content of 0%.
The mechanical properties in brief are (Inspection certificate 3.1b):

- Hardness HV30 is 221.
- Rp0.2 at RT is 552MPa
- Rp0.2 at 550°C is 358 MPa.

A detailed report (FZKA 6911) on the tensile, charpy and creep properties of EUROFER 97 is available from the Forschungszentrum Karlsruhe.

3. Specimen

A new fatigue specimen has been designed for this project. The specimen is optimized for reduced mass and gripping simplicity for the case of irradiated experiments. The cylindrical plain specimen is shown in Fig.1. It has a gauge length of 6 mm and a diameter of 2.7 mm. The length/diameter ratio is about 2.2 and the connecting radius is 12 mm. The chosen geometry should provide stability up to high total strain ranges and at high temperatures.
The specimens were cut in the L-T orientation.
The mechanical behaviour of the specimen was checked at room temperature. In monotonic tests, the geometry was still stable at a total strain range of 2% whereas after the addition of a tensile dwell the specimen became unstable at 2%.

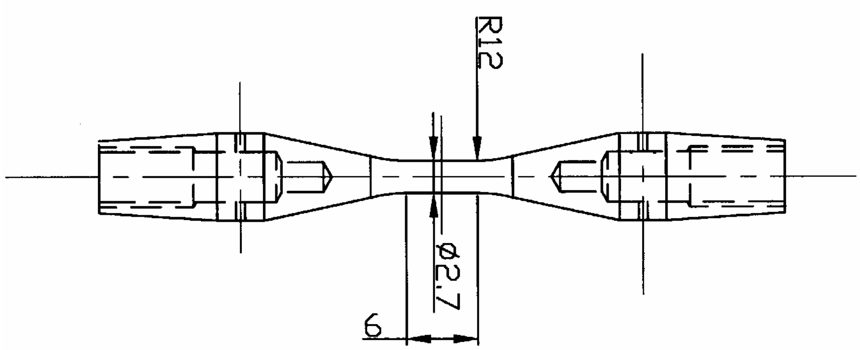

Figure 1. Eurofer fatigue specimen

The gripping shoulder which mounts with a 5mm screw on the specimen conical ends is shown in Fig.2.

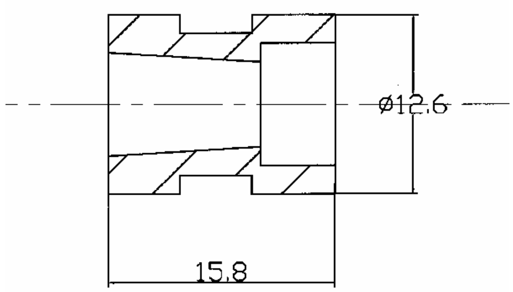

Figure 2. Shoulders to grip the specimen in the testing machine.

4. Experimental set-up

The tests were conducted with an electro-mechanical RMC100 test machine , equipped with an INSTRON electronic. The grips and the furnace were arranged inside a vacuum chamber with a minimal of pressure of 8x10-7 mbar. The displacement was measured with a manipulator-extensometer placed inside the vacuum chamber and which could be moved precisely to the specimen. The axial displacement was transmitted by two ceramic rods to a sensor equipped with strain gauges in full bridge. The tests were performed under conditions of constant total strain amplitude. The temperature of the transducer did not exceed 50°C, at the highest furnace temperature (550°C). The furnace was calibrated and controlled in relation to the temperature of the grips. A fine temperature transducer was welded onto the specimen gauge length, for all tests (see Fig. 3). The temperature of the specimen and the transducer were registered in a separate data logger, in order to get the complete temperature history of the experiment. This was necessary for safety reasons also, since some of the creep-fatigue tests lasted more than three months. The temperature history of the specimen N29F22 is shown in figure 4, as an example.

5. End of life criterion

The number of cycles to failure N_f has been determined according to the following graphical procedure shown below in Fig.5:

- A mean line is drawn onto the saturation part of the Stress to Cycle Number curve
- This line intersects with the origin (N=0) at ($\Delta\sigma=\Delta\sigma_0$)
- A parallel to this line is drawn at $\Delta\sigma=\Delta\sigma_0$-10% $\Delta\sigma_0$
- Its intersection with the tail of the Stress to Cycle Number curve, defines N_f .

This method has the advantage to work well for all FM steels, unirradiated or irradiated . Commercial softwares offer multiple different ways of stopping the test near or close to full separation of the specimen. Unfortunately, for safety reasons, the machine must be stopped before full separation and depending on the criteria used, some dispersion in the number of cycles to failure will occur.

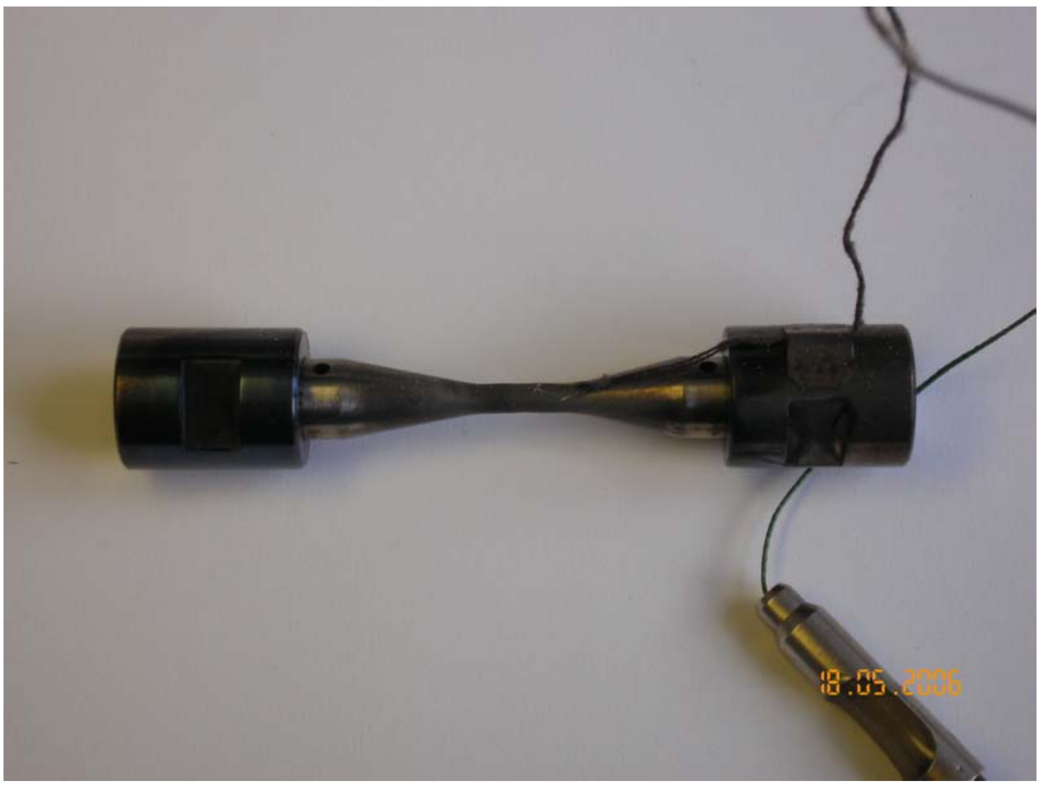

Figure 3. Specimen N29F26 shown after test. The main crack is on the left side of the gauge length.

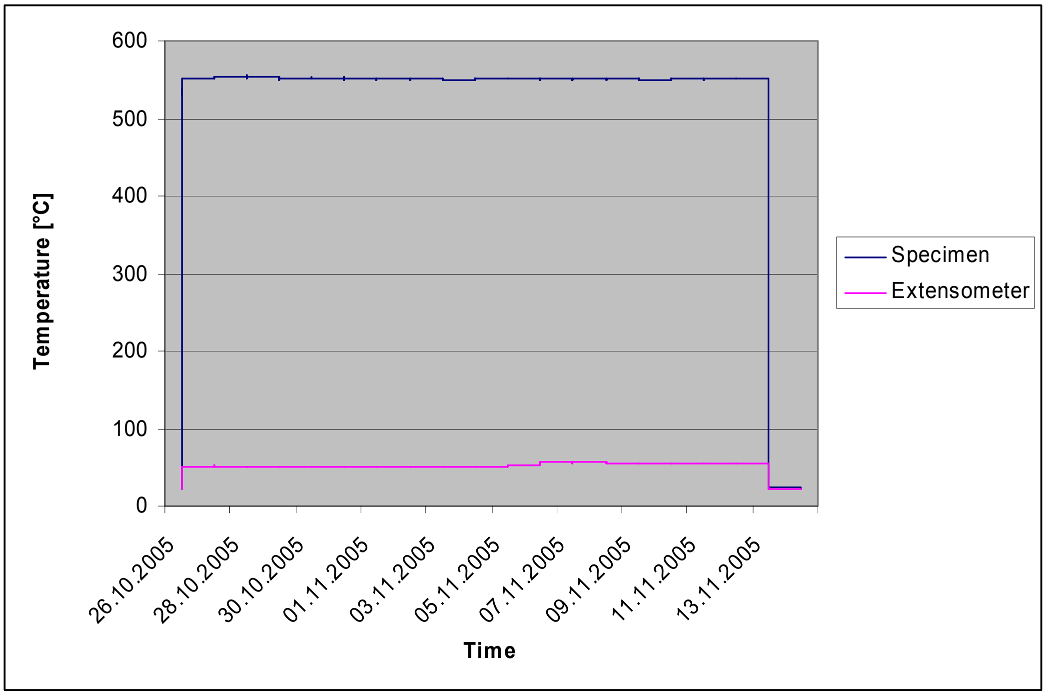

Fig. 4. Temperature history of specimen N29F22 (tested at 550°C)

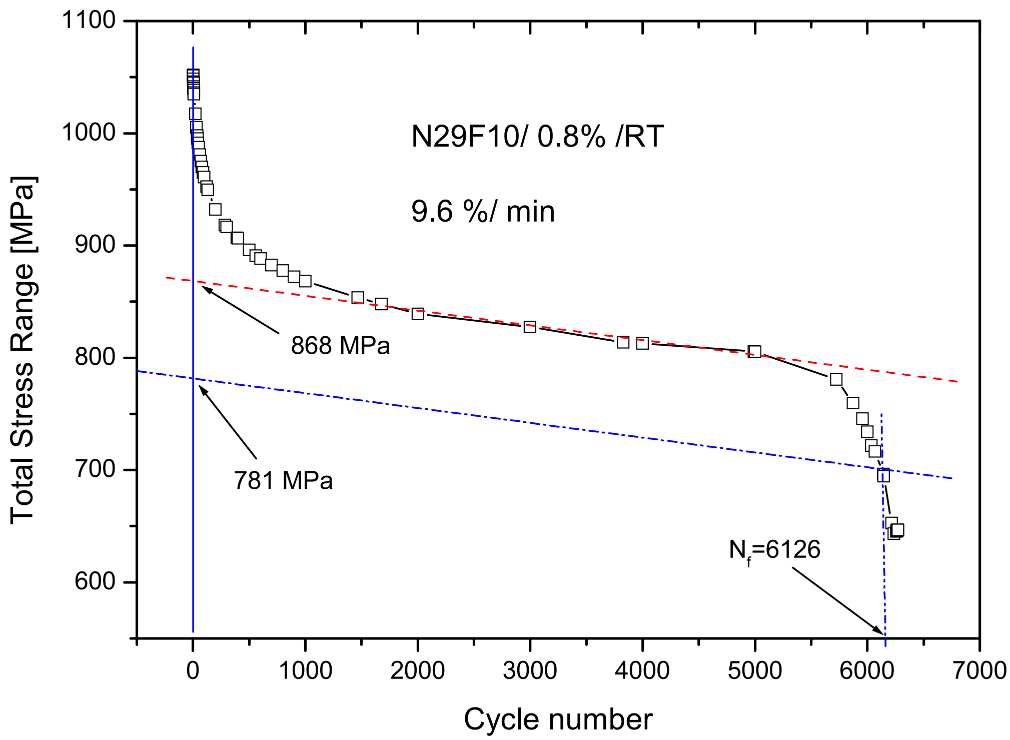

Figure 5. Graphical method for the determination of the number of cycles to failure N_f

6. Results

31 fatigue and creep-fatigue tests were performed at temperatures between RT and 550°C. The results are presented altogether in table 1, placed at the end of this report.

6.1 General Behaviour

The softening behaviour of the material corresponds to the behaviour generally observed in ferritic-martensitic steels. During the very first cycles (1-10), some little strain hardening may take place until the total stress range (the absolute difference between positive and negative stress amplitude in a cycle) shows its peak value. In most cases, the peak stress is attained in the first cycle. Only at room temperature and under low imposed strains, can this initial strain hardening phase last for a few cycles, as for specimen N29F7, tested at room temperature and at $\Delta\varepsilon_t$=0.5%, where the peak stress is attained at N=7. After this very short consolidation phase, the cyclic stress amplitude decreases very rapidly by about 20% of its initial level and then saturates to a value which then decreases very slowly as a function of the number of cycles (see Fig.5). This is called continuous softening since the material is continuously loosing its strength. As the main crack develops in the material, a pronounced decrease of the saturation stress indicates the failure of the specimen. When the failure criterion N_f is reached , the fatigue hysteresis loop has a strong inflexion point on the compression part . This is shown in Fig.6.

6.2 Room Temperature Results

The fatigue endurance measured at room temperature is shown in Fig. 7. As indicated earlier, the tests were conducted in air. The experimental points plot onto a line, probably because the plastic component of the strain is significant even at low imposed strains. One test was carried out with a tensile dwell of 500s. The fatigue life was reduced by 25%, if compared to a test run without holds. Nevertheless the effect is small and the point falls onto the mean line.

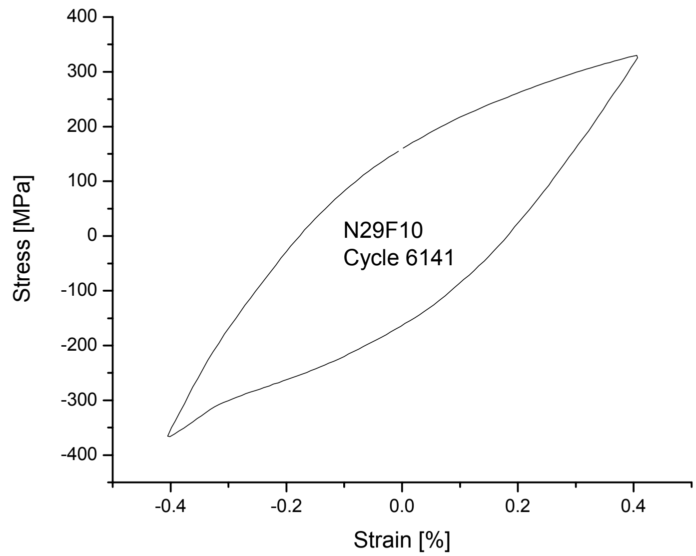

Figure 6. A typical stress-strain hysteresis loop, close to failure. N29F10, RT, $\Delta\varepsilon_t$=0.8%, N_f.=6126. The failure criterion N_f has already been reached.

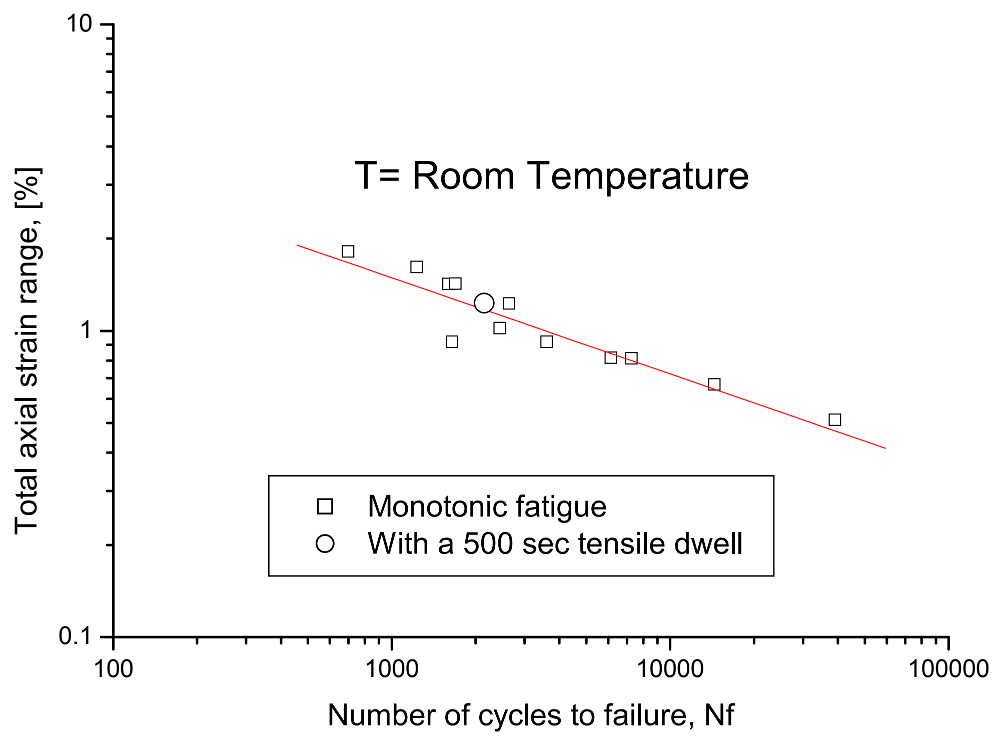

Fig. 7. Fatigue endurance at room temperature for EUROFER 97.

The room temperature data have been evaluated according to the Coffin-Manson procedure:

$$\Delta\varepsilon / 2 = \varepsilon_a = \frac{\sigma_f^{'}}{E}(2N_f)^b + \varepsilon_f^{'}(2N_f)^c \quad (1)$$

whereas the first term, the elastic strain amplitude, is simply equal to half of the difference between the total imposed strain range and the total plastic strain range. The second term of equation 1 is the plastic contribution which is equal to half of the total plastic strain range. As usual all values are taken at half life.

The total , elastic and plastic strain amplitudes of the room temperature data have been plotted in Fig. 8.

The exponent C of equation 1 has been calculated from the fit line for plastic strain and is equal to -.552. This value is closed to the values found for similar steels, see for instance reference [3].

The transition life (N_f when $\Delta\varepsilon_p/2 = \Delta\varepsilon_e/2$) is around 5200 cycles.

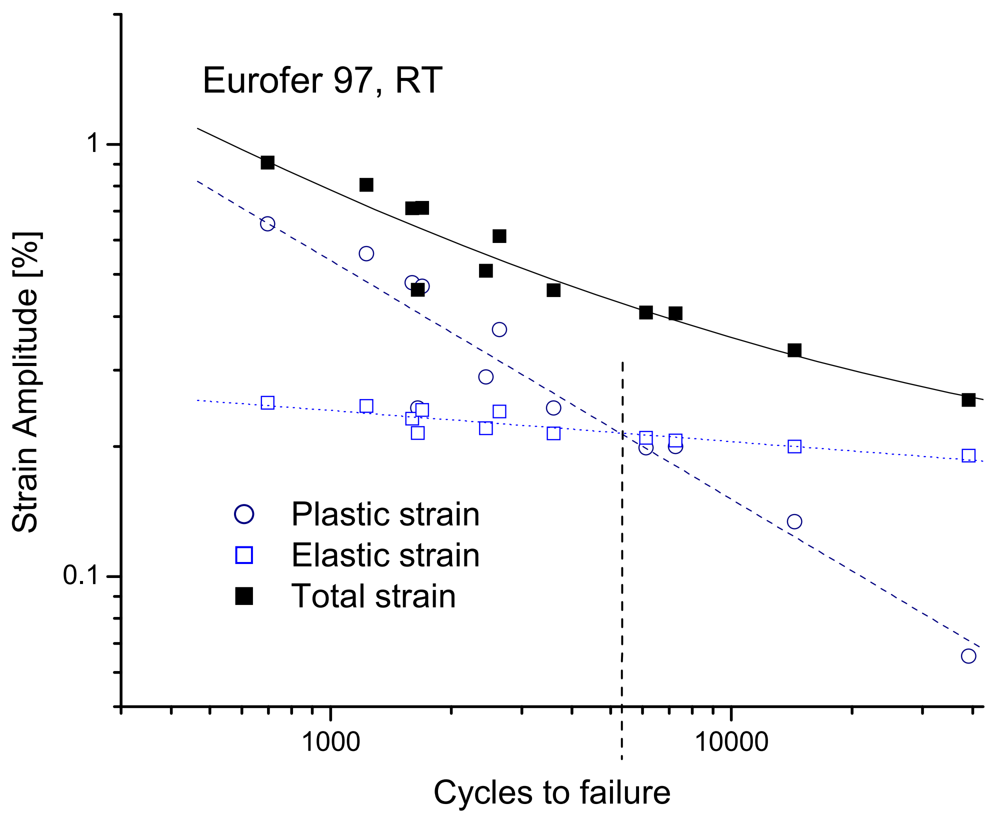

Figure 8. Strain-fatigue life response for Eurofer 97 at room temperature.

6.3 LCF at Elevated Temperatures

The fatigue endurance of Eurofer 97 at elevated temperatures is presented in figure 9. The tests were conducted in a high vacuum. The data points do not deviate strongly from the mean line. An influence of the temperature, if any, is not significant. For comparison, the mean curve of the data points obtained in air, at room temperature is also shown in Fig. 9. Even at room temperature, the negative effect of the air atmosphere is evident since the mean curve for RT data points is clearly at the left hand side of the mean curve of the high temperature results, as shown in figure 9.
In figure 10, we present the softening behaviour of the alloy, at three different temperatures, 150, 300 and 550°C. As was reported earlier by Armas et al. [4], the final stage of the cyclic softening curve appears quasi linear in a log-log scale. Therefore the final part of the softening curve (the last 80% of the cycles) can be described by the following equation:

$$\sigma_a = A \cdot N^{-s} \quad (2)$$

where σ_a is the stress amplitude, A is a constant and *s* is the cyclic softening coefficient. In Fig. 10, the softening curves for 0.8 and 0.5% total strain are shown between 150 and 550°C. It can be seen that the cyclic softening is almost identical at 150 and 300°C, but increases significantly at 550°C. Also interesting to note is that the cyclic softening does not depend on the applied strain amplitude. The larger softening observed at 550°C is an indication for some additional softening mechanism operating at the highest temperature. The measured softening coefficient s at 550°C is 0.0485. This coefficient is close to the ones observed in F82H or MANET II by Armas et al. [4].

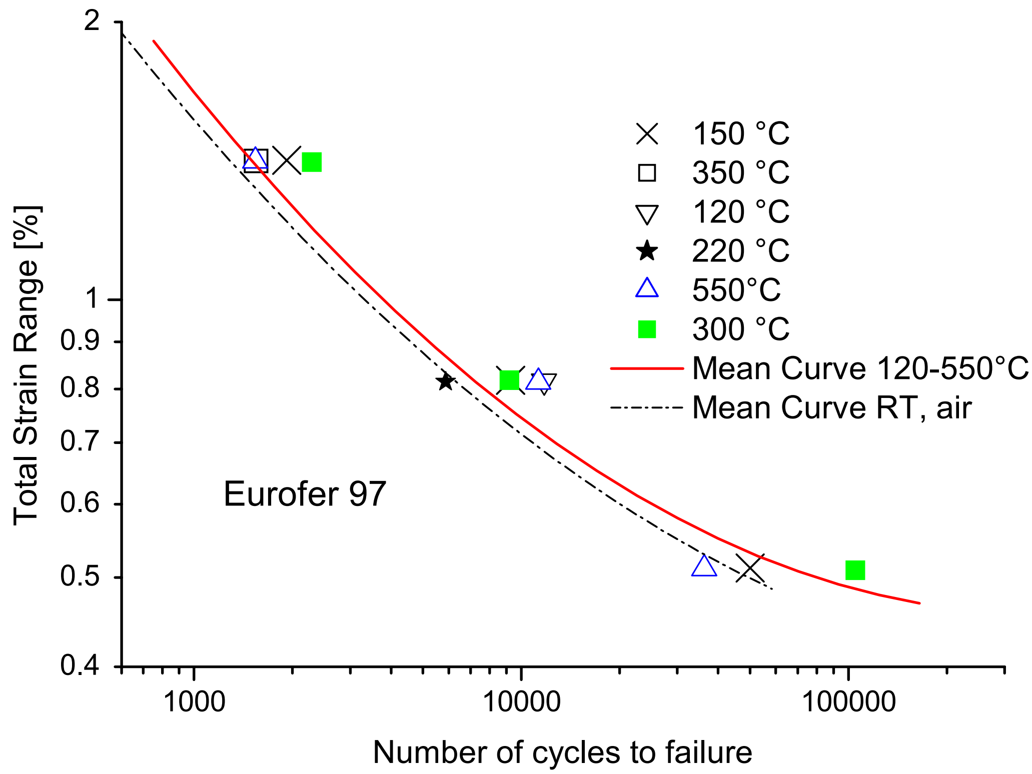

Figure 9: Fatigue performance of Eurofer 97 at elevated temperatures, in high vacuum. The mean curve of the RT results at air is shown for comparison

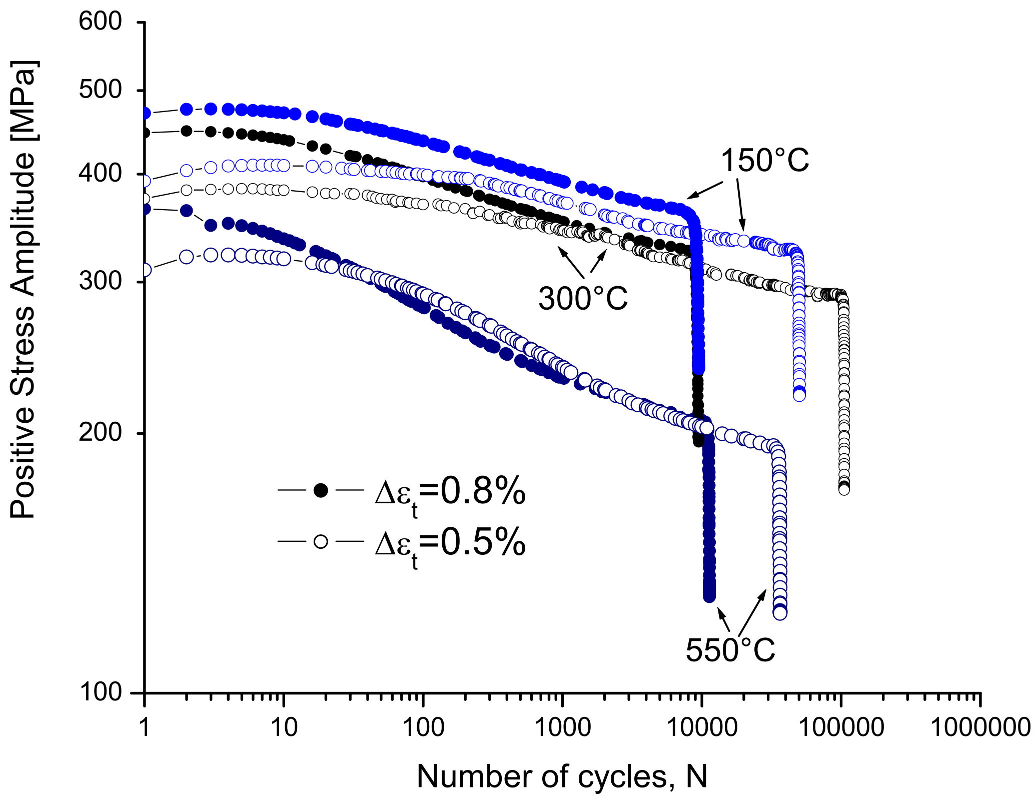

Figure 10. Softening behaviour of Eurofer 97 between 150 and 550°C.

6.4 LCF with Hold Times

Six tests have been performed, imposing a 500s dwell time at the maximum tensile strain, at 150, 300 and 550°C. Three different levels of total strain were run (see Table 1): 1.4% at all temperatures, 0.8% at 300 and 550 °C and 0.5% at 550°C.
The results are represented graphically in figure 11. It can be seen that the hold time do not affect strongly the endurance at the highest imposed strain range, at the exception of the 300°C test temperature. Nevertheless the 300°C data point would need to be repeated to see if the effect is due to some fatigue –creep interaction or if it is simply due to statistical dispersion. At 0.8% , the situation is more clear and the graphs shows a significant life reduction at the highest temperature. Finally the figure 11 c) shows a strong life reduction at 0.5% for a test temperature of 550°C. Tests at lower temperatures were not conducted because they would probably not be technically and timely achievable. The test shown in Fig.11 c) lasted for three months.

The endurance results are also shown in a classical log-log plot in Fig. 12. The effect of hold times is significant at the highest test temperature under low applied strains.

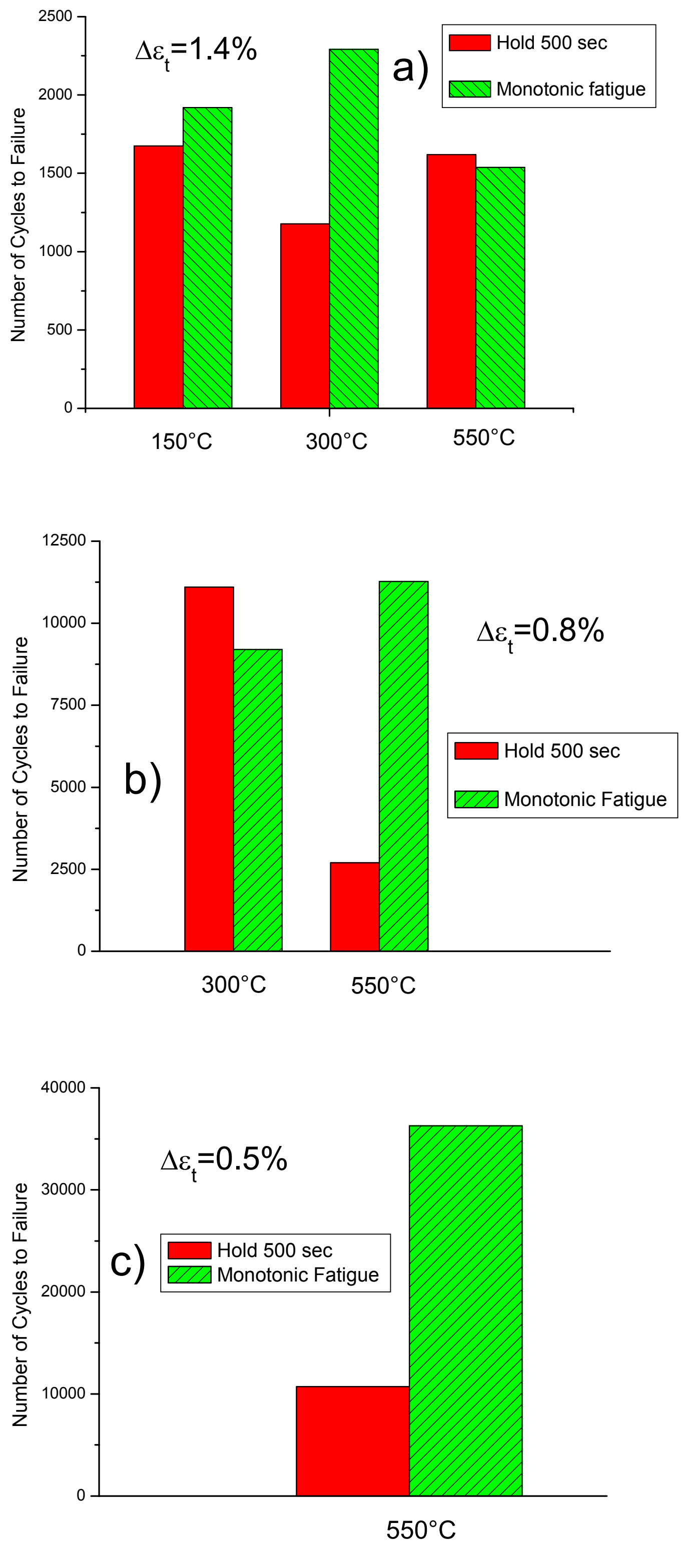

Figure 11. Column graph showing the effect of 500 sec hold times at a) 1.4%, b) 0.8% and c) 0.5% total imposed strains.

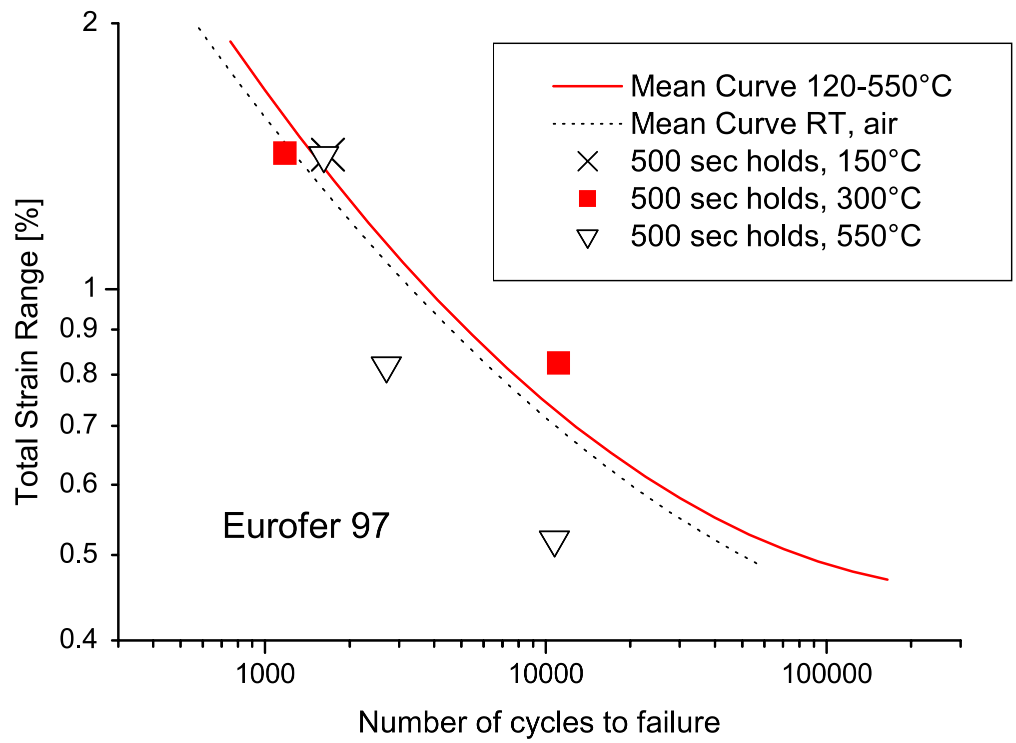

Figure 12. Endurance plot showing the effect of 500 sec hold times on fatigue life.

The softening behaviour at 550°C is shown in figure 13, for the available tests at 0.8 and 0.5%. An interesting point to make about the diagram is that the softening rate with hold times is again independent of the applied strain but at high cycles number, seems to be lower when compared to the monotonic case. Inversely, the softening rate with hold time is much stronger at the beginning of the life.
For the testing conducted with hold time, the stress level of the specimen tested at 0.5% is clearly lower than the stress level of the specimen tested at 0.8%, when compared close to end of life.
Figure14 shows some softening curves with and without hold times, at 300°C. At the lower temperature the rate of softening does not seem to be very different, with or without hold times. Another important difference at 300°C, is the much smaller difference in stress levels comparing a case with identical imposed strain, with an without an hold time. This again indicates a different materials behaviour at elevated temperature, probably because of the onset of thermal creep. This is in accordance with the fact that the hold times reduce the fatigue life effectively only at 550°C.
In figure 15, the relaxed stress for a 500 sec hold time is shown as a function of the normalized number of cycles. Each curve represents a full test. At 550°C, the curves for 0.5, 0.8 and 1.4% are converging to a common value, thus indicating that the relaxed stress at end of life is independent of the imposed strain. The comparison at 0.8% and at 300°C, indicates that at the lower temperature the relaxed stress is significantly reduced.

All curves seem to have a general behaviour very similar to the evolution of the stress range as a function of the cycles (see Fig.5): in the first cycles the relaxed stress decreases rapidly then stabilizes to a plateau and finally drops again at end of life.

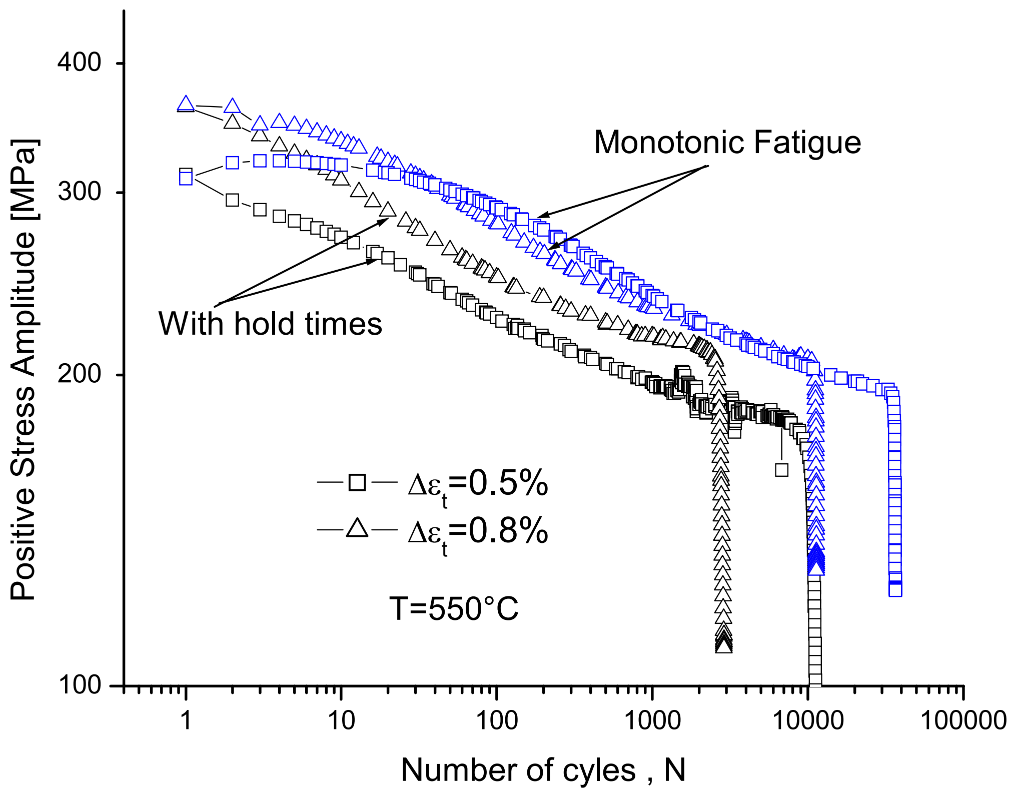

Figure 13. Comparison of the softening behaviour with and without hold times, at 550°C.

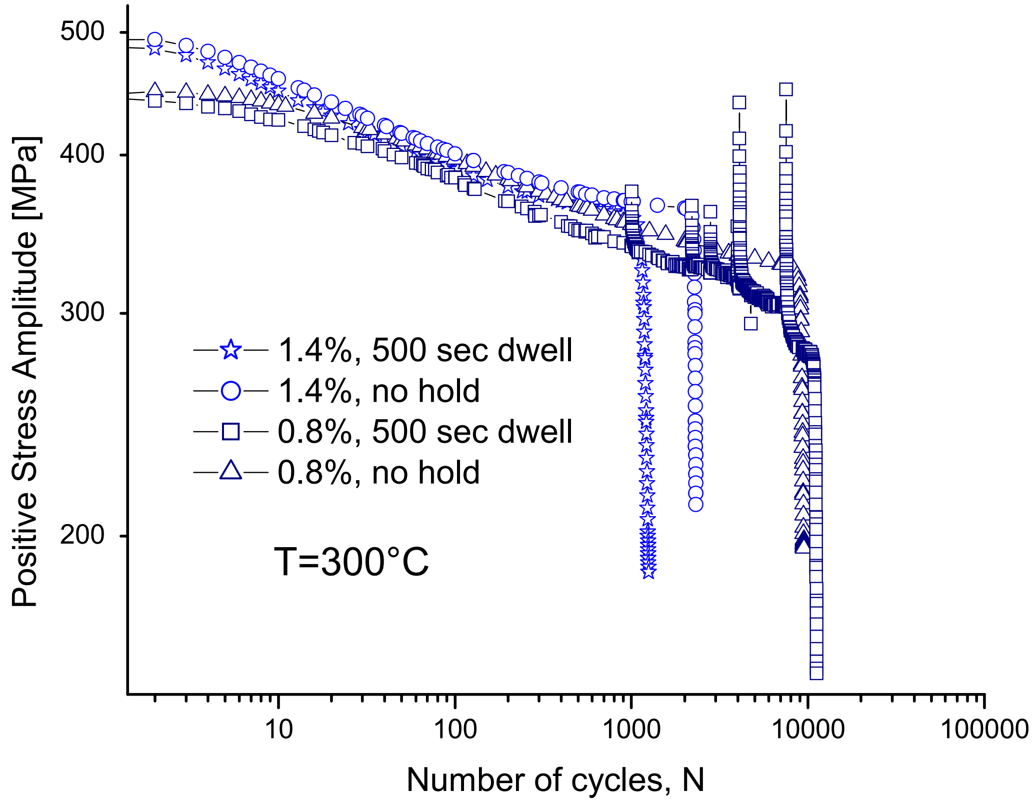

Figure 14. Comparison of the softening behaviour with and without hold times, at 300°C.

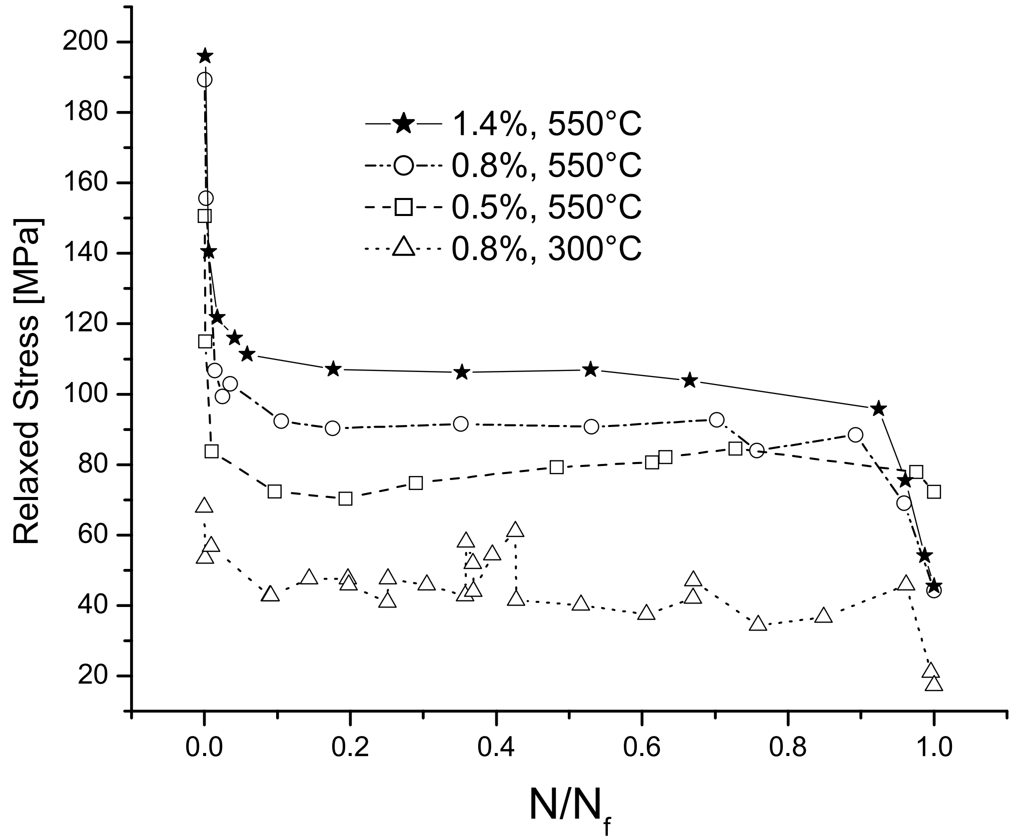

Figure15 Relaxed stress as a function of normalized number of cycles at different strain ranges and temperatures.

6.5 Analysis of Stress-Strain Hysteresis Loops

Here we will compare some stress-strain hysteresis loops in order to get information on the total amount of inelastic strain produced per cycle and on the relaxed stress, in case of tests with hold times.
In Figure 13, we have shown that at 550°C, the introduction of an hold time seems to decrease the rate of softening at the end of life. But at the beginning of life , the softening rate is more important and this is reflected also in Fig.15 , where the relaxed stress appears much higher during the first cycles. The tensile dwell and resulting relaxation seem to accelerate the softening.
Figure 16 shows the second and the cycle at half life for a specimen with hold times tested at 550°C and 1.4% (N29F21). The cycles are not fully symmetrical, at half life the positive stress is 222.6 MPa and the negative one -243 MPa. Comparing cyle number 2 and half life, the flow stress has decreased significantly and the plastic strain has

increased. The amount of relaxed stress has significantly decreased, from 200 MPa at cycle number two to 103 MPa at half life.
Figure 17 compares the curves at half life of specimens tested with and without an hold time at 500°C and 1.4% total imposed strain. Two obvious differences show up comparing both loops. First the specimen tested with the hold time has a lower tensile flow stress, second the same specimen has a larger plastic strain. The lower flow stress would normally lower the stress intensity factor at the crack, thus reducing the rate of crack propagation. On the other hand, the higher plastic flow enhances crack propagation. The resulting effect is surprisingly an improvement of the fatigue life (see Fig.11a or table 1).
Making the same comparison at a low imposed strain of 0.5%, as shown in figure 18, the situation is different because there is no visible reduction in stress(the total resulting stress range is similar) but there is a clear increase in plastic strain in the specimen with hold times. Again, the tensile dwell induces a stress asymmetry. At low imposed strains, the dwell time reduces drastically the fatigue life. The fatigue life is reduced from N_f =36'267 to N_f=10'724 (N29F26).

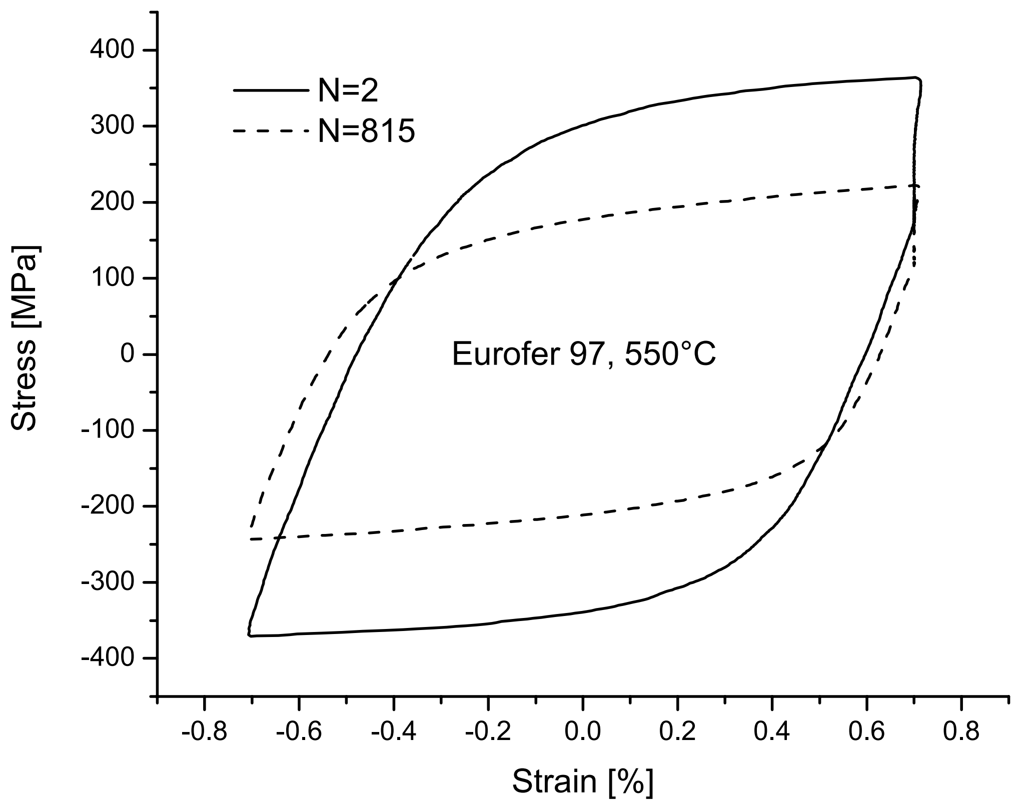

Figure16. Stress strain hysteresis loops for the 2nd and the 815th cycle (half life), at 550 °C and 1.4% total imposed strain. The amount of relaxed stress is significantly reduced at half life.

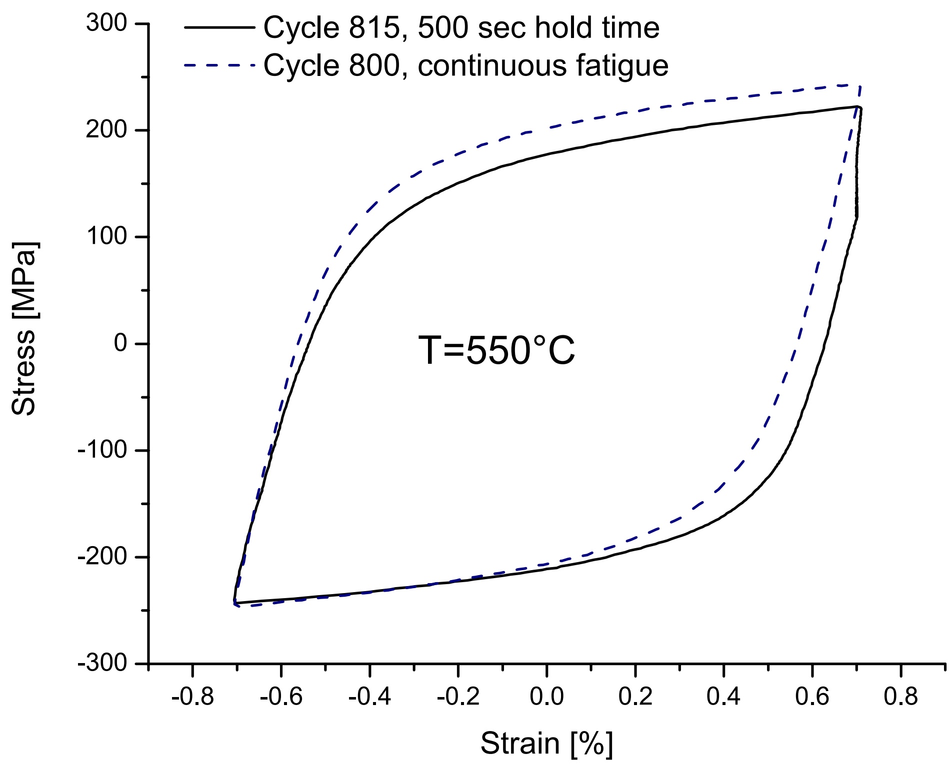

Figure17. Stress strain hysteresis loops at half life of specimens tested with and without a hold time of 500sec. The specimen tested continuously has a larger flow stress. The specimen tested with hold time has a larger plastic strain. $\Delta\varepsilon$ tot =1.4%.

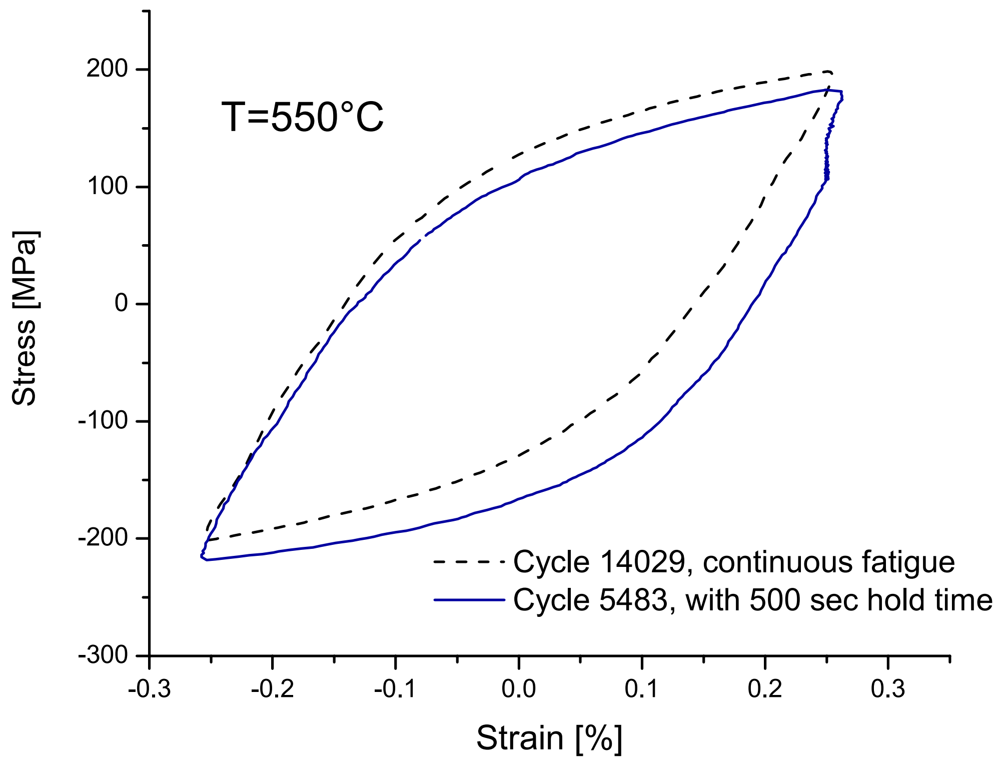

Figure18. Stress strain hysteresis loops at half life of specimens tested with and without a hold time of 500sec. The specimen tested with hold time is asymmetrical and has a larger plastic strain. $\Delta\varepsilon$ tot =0.5%.

7. Summary and Conclusions

Eurofer 97 FM steel has been tested at air, under total strain control between 0.5 and 1.8%. The room temperature fatigue properties are similar to the ones observed in other FM steels like F82H or MANET. A tensile dwell time of 500sec has only little effect on fatigue life.

The fatigue endurance at higher temperatures has been measured in high vacuum from 150 to 550°C. There is no significant effect of test temperature on fatigue life. The rate of softening appears to be independent of the applied total strain. The softening rate is independent of temperature up to 300°C, but at 550°C it becomes much higher indicating the onset of an additional softening mechanism. The measured softening coefficient at 550°C is similar to those measured in other FM steels.

At high imposed strains and at 550°C, there is no strong influence of a 500 sec hold time on fatigue life. At low imposed strains and at 550°C, there is a strong life reduction due to the introduction of the hold time.

At the beginning of life, the softening rate with hold times is much stronger as compared to the softening rate without hold times. Inversely, at the end of life, it is smaller.
The amount of stress relaxed during the dwell is independent of the applied strain, at end of life.

The analysis of the stress strain hysteresis loops has shown that the strong reduction of fatigue life observed when a tensile dwell is applied at low strains and high temperature, corresponds to a large increase of the resulting plastic strain.

Acknowledgements:

The PSI (Paul Scherrer Institue) is thanked for the technical and logistical support supplied during the testing.

Table 1. Main fatigue parameters measured in Eurofer 97. The environment is air for the room temperature tests and high vacuum for the tests at elevated temperatures.

Specimen name	T [°C]	Δε tot [%] 1/2Nf	Δε plast [%] 1/2Nf	Δε elast [%] 1/2Nf	Δσ [Mpa] 1/2Nf	Δσ peak [Mpa] (Cyc.No)	Nf	Hold [s]	Strain rate [%/min]	Environment
N29F4	20	1.815	1.31	0.505	1004	1211 (2)	697	0	21.6	air
N29F5	20	0.813	0.4	0.413	826	1048 (1)	7261	0	11.5	air
N29F7	20	0.512	0.131	0.381	745	820 (7)	39097	0	9.0	air
N29F8	20	1.421	0.957	0.464	863	1135 (1)	1600	0	16.8	air
N29F9	20	1.424	0.938	0.486	925	1164 (1)	1692	0	16.8	air
N29F10	20	0.816	0.397	0.419	3063	1052 (1)	6126	0	9.6	air
N29F13	20	1.227	0.745	0.482	897	1132 (1)	2641	0	14.4	air
N29F14	20	0.668	0.268	0.4	806	994 (3)	14401	0	11.7	air
N29F15	20	0.921	0.491	0.43	898	1070 (1)	1650	0	11.9	air
N29F31	20	0.92	0.491	0.429	837	1082 (1)	3603	0	11.9	air
N29F33	20	1.613	1.117	0.496	935	1173 (2)	1229	0	11.5	air
N29F39	20	1.02	0.579	0.441	862.5	1090 (1)	2444	0	12	air
N29F17	300	0.818	0.468	0.35	671	919 (1)	9197	0	12	vac.
N29F18	550	0.814	0.5786	0.2354	425	737 (1)	11273	0	12	vac.
N29F19	550	1.413	1.136	0.277	489	790 (1)	1538	0	12	vac.
N29F20	550	0.511	0.293	0.218	398	664(2)	36267	0	12	vac.
N29F24	120	0.816	0.448	0.368	746.5	997 (1)	11749	0	12	vac.
N29F25	220	0.815	0.473	0.342	721	944(2)	5874	0	12	vac.
N29F32	350	1.414	1.031	0.383	712	972 (1)	1547	0	12	vac.
N29F34	300	1.41	1.017	0.393	745	1010 (1)	2292	0	12	vac.
N29F35	300	0.509	0.212	0.297	591	786 (2)	105149	0	12	vac.
N29F37	150	0.512	0.192	0.32	676	842 (4)	50001	0	12	vac.
N29F38	150	0.818	0.451	0.367	740	971 (1)	9279	0	12	vac.
N29F40	150	1.416	0.99	0.426	840	1089 (1)	1920	0	12	vac.
N29F12	20	1.23	0.788	0.442	887	1151 (1)	2151	500	14.4	air
N29F16	300	1.425	1.055	0.37	744	993 (1)	1177	500	12	vac.
N29F21	550	1.417	1.23	0.187	466	869 (1)	1620	500	12	vac.
N29F22	550	0.819	0.6281	0.1909	460	746 (1)	2703	500	12	vac.
N29F23	300	0.825	0.5104	0.3146	625	905 (1)	11102	500	12	vac.
N29F26	550	0.52	0.3438	0.1762	400	656 (1)	10724	500	12	vac.
N29F36	150	1.42	1.016	0.404	837	1083 (1)	1675	500	12	vac.

References :

1. Klueh, R.L., K. Ehrlich, and F. Abe, *Ferritic/martensitic steels: promises and problems.* J. Nucl. Mater., 1992. **191-194**: p. 116-124.
2. Ehrlich, K., et al., *The development of ferritic-martensitic steels with reduced long-term activation.* J. Nucl. Mater., 1994. **212-215**: p. 678-683.
3. Victoria, M., et al. *The microstructural stability and mechanical properties of a low activation martensitic steel*. in *17th Symposium on Effects of Radiation on Materials*. 1995. Philadelphia: ASTM STP 1270.
4. Armas, A.F., et al., *Cyclic instability of martensite laths in reduced activation ferritic/martensitic steels.* J. Nucl. Mater., 2004. **329-333**: p. 252-256.
5. Aktaa, J. and R. Schmitt, *High temperature deformation and damage behavior of RAFM steels under low cycle fatigue loading: Experiments and modeling.* Fusion Engineering and Design, 2006. **81**(19): p. 2221-2231.